Available online at www.sciencedirect.com
SCIENCE DIRECT®
Journal of Sound and Vibration 266 (2003) 833–846
JOURNAL OF SOUND AND VIBRATION
www.elsevier.com/locate/jsvi

The high frequency, transient response of a panel with attached masses

R.R. Reynolds[a,*], B.D. Provencher[b], S.A. Shesterikov[c]

[a] *Adapco Ltd., 9357 General Drive, Plymouth, MI 48170, USA*
[b] *Department of Mechanical Engineering, University of Arkansas, Fayetteville, AR 72704, USA*
[c] *Department of Creep, Institute of Mechanics & Head, Moscow State University, Moscow, Russia*

Received 21 September 2001; accepted 29 September 2002

Abstract

The general, high-frequency response of a panel with attached masses is approximated using a transient form of asymptotic modal analysis (AMA). This method is derived by applying asymptotic simplifications to classical solutions in both the time and frequency domains. These relations are applied to a panel with one or more attached masses that is excited by impulsive loads. Predictions are made of the mean-squared, transverse displacement histories as well as localized responses near the added masses. It is shown that the latter compare well with experimental data when the masses are separated by more than the mean wavelength of the frequency band. The approximate solutions are shown to require relatively little computational time and memory and are applicable to general forms of excitation.

1. Introduction

High-frequency structural vibration is often a source of workplace irritation and damage to sensitive electrical equipment. While there are methods available to predict such vibrations when they are periodic or even ergodic [1–4], there are few alternatives for transient excitation sources such as collisions or impacting components [5]. Finite elements are extremely useful at low frequencies, but become cumbersome and inaccurate at high frequencies, say above 1000 Hz, where the problem is essentially modelled as wave propagation.

There have been efforts to relax the ergodic assumptions of statistical energy analysis (SEA) in order to provide some predictive capability for the transient regime [6–8]. However, results vary depending upon the assumptions made and are usually order-of-magnitude estimates.

*Corresponding author. Tel.: 734-453-2100; fax: 734-453-2543.
E-mail address: bobr@adapco.com (R.R. Reynolds).

0022-460X/03/$ - see front matter
doi:10.1016/S0022-460X(02)01449-9

A re-formulation of asymptotic modal analysis (AMA) for transient vibration has been shown to be effective for simple elastic systems such as a panel [9]. This method has been extended to the more complex geometry of a panel with attached masses [10] and this development is summarized here and verified with experimental data.

2. Governing equations

The equation of motion for a thin elastic panel with external, point forces may be written in non-dimensional form as

$$\frac{\partial^2 W}{\partial \tau^2} + C\frac{\partial W}{\partial \tau} + \left[\frac{1}{\gamma}\frac{\partial^4 W}{\partial \xi^4} + 2\frac{\partial^4 W}{\partial \xi^2 \partial \eta^2} + \gamma^2 \frac{\partial^4 W}{\partial \eta^4}\right] = P(\xi,\eta,\tau) + \lambda_0 \delta(\eta-\eta_0)\delta(\xi-\xi_0) + \lambda_1 \delta(\eta-\eta_1)\delta(\xi-\xi_1) + \cdots, \tag{1}$$

where the non-dimensionalized parameters are: the transverse displacement $W =$ displacement/thickness; the co-ordinates, $\xi = x/\text{thickness}$ and $\eta = y/\text{width}$ (cf. Fig. 1); time $\tau^2 =$ panel-bending stiffness/(density–thickness–length^2–width^2); the panel aspect ratio $\gamma =$ length/width; the structural damping, C; the applied load P at (ξ_f, η_f); and λ_i are the loads applied by R the added masses, M_i, attached to the panel at the positions (ξ_i, η_i).

A typical solution procedure is to apply Galerkin's method with an assumed displacement of the form

$$W(\xi,\eta,\tau) = \sum_{n=1}^{\infty} q_n(\tau)\psi(\xi,\eta). \tag{2}$$

This yields the uncoupled, single-mode equations

$$\frac{\partial^2 q_n}{\partial \tau^2} + 2\zeta_n \omega_n \frac{\partial q_n}{\partial \tau} + \omega^2 q_n = Q_n; \quad n = 1, 2, \ldots, \tag{3}$$

where ζ_n is the modal damping ratio, Q_n the generalized force, and ω_n is the natural frequency

$$\omega_n = \left(\frac{\pi^2}{\gamma}\right)[n_x^2 + n_y^2\gamma^2]. \tag{4}$$

Here n_ξ and n_η are the modal indices in the co-ordinate directions.

2.1. Classical solution for a point excitation

Now for the sake of clarity, consider a localized load at the point (ξ_f, η_f). The applied pressure becomes $P(\xi,\eta,\tau) = f(\tau)\delta(\xi-\xi_f)\delta(\eta-\eta_f)$ (cf. Fig. 1), and the generalized force can be written as

$$Q_n = \frac{\int_A (P + \lambda_0 \delta_{\xi_0}\delta_{\eta_0} + \lambda_1 \delta_{\xi_1}\delta_{\eta_1} + \cdots)\psi_n \, \mathrm{d}A}{\int_A \psi_n^2 \, \mathrm{d}A} \tag{5}$$

$$= \frac{f\psi_{nf} + \lambda_0 \psi_{n0} + \lambda_1 \psi_{n1} + \cdots}{\langle \psi_n^2 \rangle}, \tag{6}$$

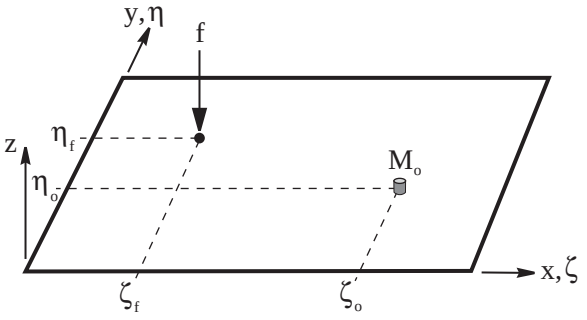

Fig. 1. Geometry of a panel, load and a single, attached mass.

where $\langle \cdots \rangle$ indicates the spatial average and the modal function at the ith mass, $\psi(\xi_i, \eta_i)$, is abbreviated as ψ_{ni}. This is used to determine the modal coefficients from

$$q_n(\tau) = \int_0^\tau h_n(\tau - \tau') Q_n(\tau') \, \mathrm{d}\tau', \tag{7}$$

where h_n is the standard impulse response function,

$$h_n(\tau) = \frac{\mathrm{e}^{-\zeta_n \omega_n \tau} \sin(\omega_n \sqrt{1 - \zeta_n^2}\tau)}{\omega_n \sqrt{1 - \zeta_n^2}}. \tag{8}$$

In this case, the modal coefficients are

$$q_n(\tau) = \frac{1}{\langle \psi_n^2 \rangle} \{ h_n(\tau) * [f(\tau)\psi_{nf} + \lambda_0(\tau)\psi_{n0} + \lambda_1(\tau)\psi_{n1}] + \cdots \}. \tag{9}$$

where $*$ indicates the convolution. The Lagrange multipliers, λ_i, are found from the equations of motion for the added masses, M_i,

$$\lambda_i(\tau, \xi_i, \eta_i) = -M_i \ddot{W}(\xi_i, \eta_i) \tag{10}$$

$$= -M_i \sum \ddot{q}_n(\tau)\psi_{ni}, \tag{11}$$

where the dots indicate derivatives with respect to non-dimensional time, τ. The $\ddot{q}_n(\tau)$ are determined by differentiating Eq. (9) twice with respect to τ. Substituting this into Eq. (11) results in a series of implicit, simultaneous equations for the λ_i in terms of the forcing, $f(\tau)$, and the modal impulse response functions, $h_n(\tau)$. However, an *explicit* relation for the forces may be obtained by transforming them to the frequency domain and employing the convolution theorem.

Performing this substitution and transformation using the common form of the convolution theorem, $\mathscr{F}(f * g) = \sqrt{2\pi}\mathscr{F}(f) \cdot \mathscr{F}(g)$,[1] it is helpful to employ the transform relation $\mathscr{F}[\ddot{h}_n(\tau)] =$

[1] The Fourier transform is used here rather than the Laplace for numerical efficiency. It is

$$G(\omega) = \mathscr{F}[g(\tau)] = \frac{1}{\sqrt{2\pi}} \int_{-\infty}^{\infty} \mathrm{e}^{-i\omega\tau} g(\tau) \, \mathrm{d}\tau. \tag{12}$$

$-\omega^2\sqrt{2\pi}H_n(\omega)$. Using the notation $\Lambda_0(\omega)=\mathscr{F}[\lambda_0(\tau)]$, $H_n(\omega)=\mathscr{F}[h_n(\tau)]$, and $F(\omega)=\mathscr{F}[f(\tau)]$, this yields the transformed Lagrange multipliers for the ith mass,

$$\Lambda_i(\omega,\xi_i,\eta_i) = -M_i\sum\frac{\psi_{ni}}{\langle\psi_n^2\rangle}\Bigg\{F(\omega)\psi_{nf}(1-\omega^2\sqrt{2\pi}H_n(\omega)) + \sum_{j=0}^{R}\Lambda_j(\omega,\xi_j,\eta_j)\psi_{nj}(1-\omega^2\sqrt{2\pi}H_n(\omega))\Bigg\}. \tag{13}$$

This system of equations may be rearranged in the more convenient form

$$\mathbf{A}\vec{\Lambda}=\vec{M}, \tag{14}$$

where the elements of the symmetric $\mathbf{A}$ are

$$a_{ii}=1+M_i\sum\frac{\psi_{mi}^2}{\langle\psi_m^2\rangle}(1-\omega^2\sqrt{2\pi}H_m(\omega)), \tag{15}$$

$$a_{ij}=M_j\sum\frac{\psi_{mi}\psi_{mj}}{\langle\psi_m^2\rangle}(1-\omega^2\sqrt{2\pi}H_m(\omega)), \tag{16}$$

and the elements of $\vec{M}$ are

$$m_i=-F(\omega)M_i\sum\frac{\psi_{mi}\psi_{mf}}{\langle\psi_m^2\rangle}(1-\omega^2\sqrt{2\pi}H_m(\omega)). \tag{17}$$

We emphasize again that Eq. (14) is explicit for the Λ_i—the transformed Lagrange multipliers. Its solution provides the multipliers for the transformed modal coefficients (i.e., the transform of Eq. (9)),

$$\mathscr{F}(q_n)=\frac{\sqrt{2\pi}H_n(\omega)}{\langle\psi_n^2\rangle}\left[F(\omega)\psi_{nf}+\sum_{j=0}^{R}\Lambda_j(\omega,\xi_j,\eta_j)\psi_{nj}\right]. \tag{18}$$

This may be inverted and substituted into Eq. (2) to determine the transverse panel deflection. Restricting attention to a range of frequencies $\Delta\omega$ that contains ΔM modes yields the classical, band-limited response

$$W(\xi,\eta,\tau)=\sum_{n=M}^{M+\Delta M-1}\frac{\psi_n(\xi,\eta)}{\langle\psi_n^2\rangle}\left[k_{nF}(\tau)\psi_{nf}+\sum_{j=0}^{R}k_{n\Lambda_i}(\tau,\xi_i,\eta_i)\psi_{ni}\right], \tag{19}$$

where

$$k_{nF}(\tau)=\mathscr{F}^{-1}[\sqrt{2\pi}H_n(\omega)F(\omega)], \tag{20}$$

$$k_{n\Lambda_i}(\tau,\xi_i,\eta_i)=\mathscr{F}^{-1}[\sqrt{2\pi}H_n(\omega)\Lambda_i(\omega,\xi_i,\eta_i)]. \tag{21}$$

The spatial mean-squared response, $\langle W^2(\tau)\rangle$, can be found by first squaring Eq. (19) (neglecting the cross-terms as they are small) and spatially averaging this over the panel. This

procedure yields

$$\langle W^2(\tau)\rangle = \sum_{n=M}^{M+\Delta M-1} \frac{1}{\langle \psi_n^2\rangle}\left[k_{nF}(\tau)\psi_{nf} + \sum_{j=0}^{R} k_{n\Lambda_i}(\tau,\xi_i,\eta_i)\psi_{ni}\right]^2, \tag{22}$$

which describes the mean temporal response of the entire panel.

2.2. Asymptotic solution for a point excitation

While these solutions are straightforward, they require solving for the eigenvalues and eigenvectors of the system—a non-trivial task at high frequencies. It is far more practical to note that the modal density is quite large at high frequencies and that the response is, therefore, a result of the aggregate of the modal responses. This suggests that an asymptotic limit for the modal behavior may be a useful and more easily calculated alternative.

If the frequency range $\Delta\omega$ contains enough modes with a sufficient modal density, then several simplifications may be applied to the classical solutions of Eqs. (19) and (22). These steps eliminate the need to solve the eigenproblem and substantially reduce the size of the summations. The result is an approximate solution that is simpler to evaluate, requires much less detailed information about the system and retains the essential character and magnitude of the response.

Begin with the summation in the diagonal elements of **A** (cf. Eq. (15)). For the frequency band from modes M to $M+\Delta M$ this is

$$\sum_{m=M}^{M+\Delta M} \frac{\psi_{mi}^2}{\langle \psi_m^2\rangle}(1-\omega^2 H_m(\omega)). \tag{23}$$

Within the frequency range $\Delta\omega$ note that $H_m(\omega)$ is *not* slowly varying over the range of the summation and cannot be removed from the summation. Thus, the asymptotic modal approximations used for the smooth panel [2,9] cannot be applied here. However, two useful observations are

- The scaling factor ψ_{mi}^2 ranges from zero to one throughout the frequency range.
- The term $\left(1-\omega^2 H_m(\omega)\right)$ is a frequency-dependent function in two senses. First, for any value of m, it is multiplied by a continuous function of ω. Also, the m subscript indicates a dependence upon the natural frequency of the mth mode.

The first observation suggests that ψ_{mi}^2 may be eliminated by approximating its *scaling effect* on the H_m terms. If ΔM is large enough then we only need to sum a few, say ΔM^*, representative terms of the complete summation. This will be true if H_m is a well behaved and smoothly varying function throughout the range of the summation.

This leads us to the second observation: that the natural frequency content of H_m must be considered in any attempt to remove specific eigensolution references from the summation. The

transform of H_m is

$$H(\omega) = \frac{1}{(\omega_n^2 - \omega^2) - \mathrm{j}(2\zeta\omega_n\omega)}, \tag{24}$$

where $\mathrm{j} = \sqrt{-1}$ and ω_m is the natural frequency of the mth mode. Note that this is a smooth function of ω_m and ω. Thus, the frequency dependence of the complete summation may indeed be approximated by summing a few functions, $H_p(\omega)$, that are based on chosen frequencies, ω_p, distributed throughout $\Delta\omega$ rather than the natural frequencies.

To summarize the process:

1. Extract $\psi_{mi}^2/\langle\psi^2\rangle$ from each term and scale the complete summation by its mean value, $\bar{\psi}_{mi}^2$.
2. Reduce the number of terms in the summation from ΔM to some fraction of it, $\Delta M^* = \alpha\Delta M$, where α is a chosen parameter (typically 0.1–0.2), and scale the sum accordingly.
3. Replace the natural frequency dependence of H_m with specified frequencies that span the frequency range $\Delta\omega$ in some sense.

With these modifications the summation becomes

$$\sum_{m=M}^{M+\Delta M} \frac{\psi_{mi}^2}{\langle\psi_m^2\rangle}(1 - \omega^2 H_m(\omega)) \approx \frac{1}{\alpha} \sum_{p=M}^{M+M^*} (1 - \omega^2 H_p(\omega)), \tag{25}$$

where the $\Delta M^* = \alpha\Delta M$ chosen frequencies replace the natural frequencies in $H_p(\omega)$ and we observe that the spatial average of a mode squared is equal to the mean value of a summation of modes squared at any location (i.e., $\bar{\psi}^2(\xi_i, \eta_i) \approx <\psi^2>$). Relations for estimating ΔM are available in the literature for many continuous structures [1].

The validity of the approximations in Eq. (25) may be seen by comparing both sides of the equation for a representative system. Fig. 2 presents a comparison of two sides of Eq. (25): the CMA and AMA solutions or left and right hand sides, respectively. These calculations were made using a value of $\alpha = 0.1$ or with 10% of the estimated number of modes in $\Delta\omega$.[2] The transforms of the summations have been inverted so that the comparison can be made in the time domain. It should be noted that the AMA approximation required only 7% of the computational time necessary for the CMA calculation.

Now consider the different summations in the off-diagonal terms of $\mathbf{A}$ in Eq. (16) and the elements of $\vec{M}$ in Eq. (17). The summations in these terms have the form

$$\sum_{m=1}^{M} \frac{\psi_{mi}\psi_{mj}}{\langle\psi_m^2\rangle}(1 - \omega^2 H_m(\omega)). \tag{26}$$

The simplifications applied above to the diagonal terms are not applicable here since the eigenmode scaling is not a mode squared but rather a product of mode functions that are, in general, evaluated at different locations, $\psi_{mi}\psi_{mj} = \psi_m(\xi_i, \eta_i)\psi_m(\xi_j, \eta_j)$. Clearly this product can be

[2] Other parameters include $v = 0.359, \gamma = 1.21429, \zeta = 0.001, \omega_{min} = 769.64, \Delta\omega = 1172.93$. The excitation used is a the strike of an impulse hammer

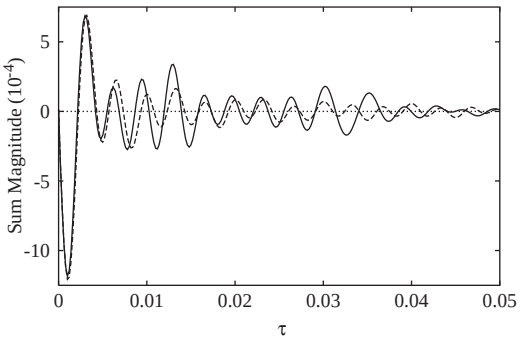

Fig. 2. Comparison of the CMA summation on the left side of Eq. (25) (solid line) to the AMA approximation on the right side of the equation (dashed line). The AMA approximation only uses 10% of the estimated modes in the frequency range (i.e., $\alpha = 0.1$).

either positive or negative. Furthermore, the asymptotic limit of the product is zero,

$$\lim_{\Delta M \to \infty} \psi_{mi}\psi_{mj} = 0. \tag{27}$$

Fortunately, the actual summation is over a finite number of modes and will only be *nearly* zero. This is an important distinction for a zero value for this summation would imply that the response of the plate is independent of the added mass, M_i. As this cannot be true, the non-zero value of the summation in Eq. (26), however small, is crucial.

To approximate this summation we extract $\psi_{mi}\psi_{mj}$ from each term and multiply the sum by the mean value of the product over the frequency range, $\bar{\psi}_{ij}$. Again, we abbreviate the summation to $\Delta M^* = \alpha \Delta M$ terms that are based on chosen frequencies that span the frequency range $\Delta\omega$. Together these steps result in the relation

$$\sum_{m=M}^{M+\Delta M} \frac{\psi_{mi}\psi_{mj}}{\langle \psi_m^2 \rangle}(1 - \omega^2 H_m(\omega)) \approx \frac{\bar{\psi}_{ij}}{\alpha \langle \psi^2 \rangle} \sum_{p=M}^{M+M^*} (1 - \omega^2 H_p(\omega)). \tag{28}$$

Here $\bar{\psi}_{ij} \approx\!\approx \langle \psi^2 \rangle$, but must be *estimated*. For sufficiently large ΔM one may use the continuous approximation

$$\bar{\psi}_{ij} = \frac{\sum_{i=M}^{M+\Delta M} \psi_{ni}\psi_{nj}}{\Delta M} \approx \frac{\int_{N_{\Delta\omega}} \psi_{ni}\psi_{nj}}{N_{\Delta\omega}}, \tag{29}$$

where $N_{\Delta\omega}$ is the number of modes in the frequency range $\Delta\omega$. This is a tedious but straightforward integration in mode-number space that yields a mean value for the cross-product for the particular frequency range, $\Delta\omega$. This is discussed more thoroughly in Appendix A.

Once the Λ_i are known, the time-domain coefficients $k_{i\Lambda_i}$ are determined and used with Eq. (19) for the panel displacement or Eq. (22) for $\langle W^2 \rangle$. These relations contain summations over the modes that can also be simplified. Since k_{iF} and $k_{i\Lambda_i}$ are time varying, they may be approximated using the asymptotic simplifications used for a smooth panel [9]. Applying these yields the

displacement relation

$$W(\xi,\eta,\tau)\approx\frac{1}{\alpha\langle\psi^2\rangle}\sum_{p=M}^{\Delta M^*}\psi_p(\xi,\eta)\left[k_{pF}(\tau)\psi_{pf}+\sum_{j=0}^{R}k_{p\Lambda_j}^{AMA}(\tau,\xi_j,\eta_j)\psi_{pj}\right]. \tag{30}$$

Although $k_{pF}(\tau)$ itself is not different in form than the analogous term in the classical solution of Eq. (19), the summation is abbreviated and the terms are evaluated at the fewer, chosen frequencies rather than the full range of natural frequencies.

Eq. (30) contains a series of products of the modal functions at the forcing and mass locations, $\psi_{pf}\psi_{pj}$, which cannot be evaluated without the eigensolution. Hence the same form of modal averaging used in Eq. (29) must be applied and attention focused on the response of the panel near the locations of the masses or the forcing. The response at other locations may be estimated using the spatial, mean-squared response discussed below. The asymptotic response near the excitation for R added masses is then

$$W_{AMA}(\xi_f,\eta_f,\tau)=\frac{1}{\alpha}\sum_{p=M}^{M+\Delta M^*}\left[k_{pF}(\tau)+\sum_{i=1}^{R}k_{p\Lambda_i}^{AMA}(\tau,\xi_i,\eta_i)\left(\frac{\bar{\psi}_{if}}{\langle\psi^2\rangle}\right)\right] \tag{31}$$

and near the mass M_i is

$$W_{AMA}(\xi_n,\eta_n,\tau)=\frac{1}{\alpha}\sum_{p=M}^{M+\Delta M^*}\left[k_{p\Lambda_n}^{AMA}(\tau,\xi_n,\eta_n)+k_{pF}(\tau)\left(\frac{\bar{\psi}_{nf}}{\langle\psi^2\rangle}\right)+\sum_{i=1,\neq n}^{R}k_{p\Lambda_i}^{AMA}(\tau,\xi_i,\eta_i)\left(\frac{\bar{\psi}_{in}}{\langle\psi^2\rangle}\right)\right]. \tag{32}$$

The case of a coincident mass and force is easily handled by noting that $\bar{\psi}_{if}=\langle\psi^2\rangle$.

2.3. Asymptotic, mean-squared response

The asymptotic limit of the spatial, mean-squared response is formed in a manner similar to that of Eq. (32). Squaring Eq. (30) and applying the same asymptotic steps yields

$$\langle W_{AMA}^2(\tau)\rangle\approx\frac{1}{\alpha}\sum_{p=M}^{M+\Delta M^*}\left\{k_{nF}^2(\tau)+\sum_{i=1}^{R}\left[k_{n\Lambda_i}^2(\tau,\xi_i,\eta_i)+2k_{nF}(\tau)k_{n\Lambda_i}(\tau,\xi_i,\eta_i)\frac{\bar{\psi}_{fi}}{\langle\psi^2\rangle}\right]+\sum_{i,j=1;i\neq j}^{R}k_{n\Lambda_i}(\tau,\xi_i,\eta_i)k_{n\Lambda_j}(\tau,\xi_j,\eta_j)\frac{\bar{\psi}_{ij}}{\langle\psi^2\rangle}\right\}. \tag{33}$$

The relations described above predict the mean-squared panel response or the panel response at the locations where a point load is applied or added masses are attached. They require none of the natural frequencies or modes of the panel and are valid for arbitrary forms of excitation. Furthermore, they require substantially less computational effort than the classical solutions of Eqs. (19) and (22).

Care is required when selecting the frequency distribution for the asymptotic solution. Evenly spaced frequencies impose a prominent beat to the response and random frequency spacing is inappropriate for reasons not the least of which is repeatability. Experience indicates that a nominally even spacing with a superimposed perturbation (say, 20–30%) is effective. Furthermore, the same chosen frequencies should not be used for the diagonal and off-diagonal elements of matrix **A** as this leads to a trivial solution.

3. Experimental verification

To confirm the asymptotic relations presented above, a simple panel was instrumented with either an accelerometer alone or an accelerometer with an additional mass attached. These configurations represented an attached mass of two different sizes. The panel was struck with an impulse hammer and the transient accelerometer and force data was low-pass filtered and recorded.

The panel used was aluminum with the physical parameters: length = 0.864 m, width = 0.711 m, ($\gamma = 1.214$), thickness = 0.00318 m, and a modal damping of approximately $\zeta = 0.005$ was used to account for the structural and acoustic losses. The elastic modulus was 73 GPa, the density was 2800 kg/m^3, and the Poisson ratio $v = 0.359$. The accelerometer mass alone was 2.1 g ($M_0 = 2.36 \times 10^{-4}$) and with an additional mass was a total of 14.6 g ($M_0 = 1.64 \times 10^{-3}$). The mass was attached to the panel at the location $(\xi_0, \eta_0) = (\frac{1}{\pi}, \frac{1}{\pi})$ and the impulse hammer strike was approximately at the location of the masses.

The response was sampled and band-pass filtered in the frequency domain using a flat, acausal filter. Two frequency ranges are considered: 1020–2653 Hz (125–325 non-dimensional Hertz) and 1837–3470 Hz (225–425 non-dimensional Hertz). Each of these ranges contained approximately 100 modes. These data were compared to AMA predictions of the local panel acceleration calculated using the force data that was captured from the impulse hammer. Thus, the forcing functions for both experiment and AMA prediction were the same. The comparisons of these responses are shown in Figs. 3–6.

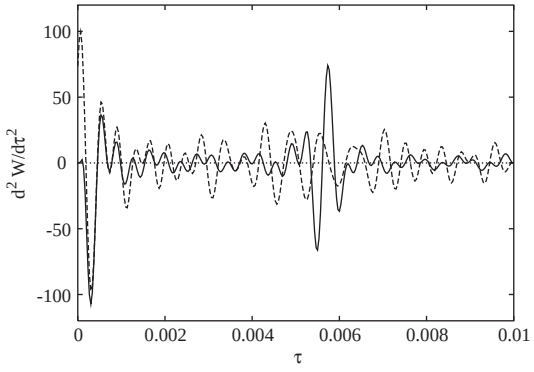

Fig. 3. Comparison of the asymptotic modal analysis prediction of panel accelerations, $\langle \ddot{W}^2 \rangle$ (solid line), with experimental data (dashed line). An added mass to the panel was given an impulsive excitation at $M_o = 2.36 \times 10^{-4}$ and was attached at the point of excitation, $(\xi_f, v_f) = (\frac{1}{\pi}, \frac{1}{\pi})$. The frequency range of the data is 125–325 non-dimensional Hertz and the AMA approximation only used 10% of the estimated modes in the frequency range (i.e., $\alpha = 0.1$).

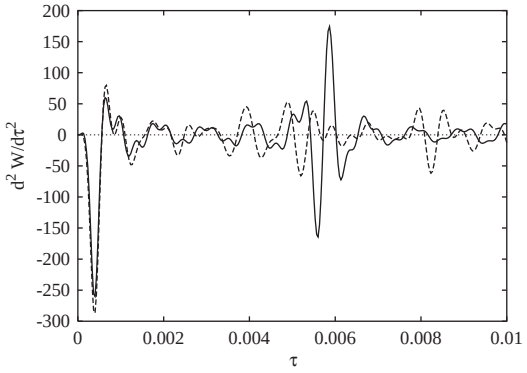

Fig. 4. Comparison of the asymptotic modal analysis prediction of panel accelerations, $\langle \ddot{W}^2 \rangle$ (solid line), with experimental data (dashed line). An added mass to the panel was given an impulsive excitation at $M_o = 1.64 \times 10^{-3}$ and was attached at the point of excitation, $(\xi_f, v_f) = (\frac{1}{\pi}, \frac{1}{\pi})$. The frequency range of the data is 125–325 non-dimensional Hertz and the AMA approximation only used 10% of the estimated modes in the frequency range (i.e., $\alpha = 0.1$).

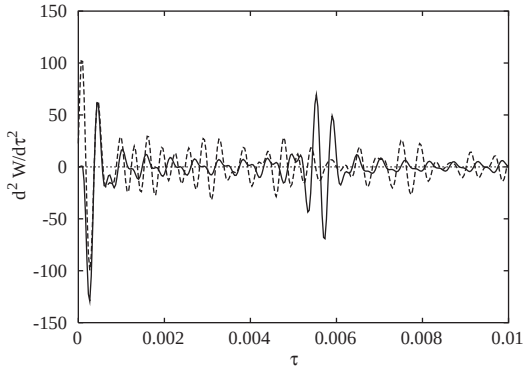

Fig. 5. Comparison of the asymptotic modal analysis prediction of panel accelerations, $\langle \ddot{W}^2 \rangle$ (solid line), with experimental data (dashed line). An added mass to the panel was given an impulsive excitation at $M_o = 2.36 \times 10^{-4}$ and was attached at the point of excitation, $(\xi_f, v_f) = (\frac{1}{\pi}, \frac{1}{\pi})$. The frequency range of the data is 225–425 non-dimensional Hertz and the AMA approximation only used 10% of the estimated modes in the frequency range (i.e., $\alpha = 0.1$).

Fig. 3 displays the comparison of AMA and experimental values for the panel acceleration in the low-frequency range (125–325 non-dimensional Hertz). It shows that the AMA approximation quite accurately predicts the amplitude and general shape of the panel response. It should be noted that the experimental data does not start at $W = 0$ as one might expect due to distortion from the acausal filter used. This filter was used because it preserved most of the initial magnitude information of the signal. Several common, causal filters were also tried, but they distorted the signal far too much to be useful. This was particularly evident near $t = 0$ where the amplitude is largest and, therefore, of the greatest importance. The behavior of the filters was evaluated using classical solutions alone before being compared to the AMA solutions.

The other difference between the solutions occurs near $t = 0.0055$ where the AMA prediction overestimates the response. This is a beat phenomenon that results from the limited number of

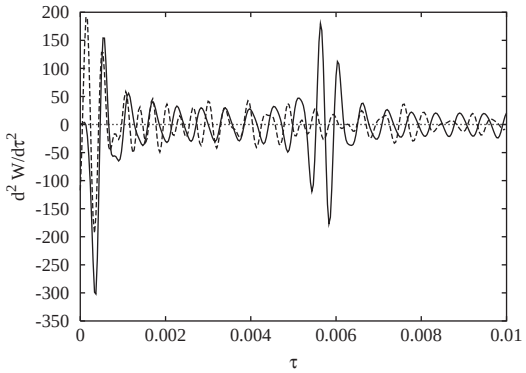

Fig. 6. Comparison of the asymptotic modal analysis prediction of panel accelerations, $\langle \ddot{W}^2 \rangle$ (solid line), with experimental data (dashed line). An added mass to the panel was given an impulsive excitation at $M_o = 1.64 \times 10^{-3}$ and was attached at the point of excitation, $(\xi_f, v_f) = (\frac{1}{\pi}, \frac{1}{\pi})$. The frequency range of the data is 225–425 non-dimensional Hertz and the AMA approximation only used 10% of the estimated modes in the frequency range (i.e., $\alpha = 0.1$).

frequencies used in the AMA summations. This was noted earlier and is a periodic error that is easily identified in the response [9,10].

Fig. 4 displays a similar comparison using the heavier attached mass. Again the large, initial response is well predicted by the AMA relations and the general decay of the two responses are similar. As with any structural dynamic calculation, the decay envelope is highly dependent upon the damping values chosen. Thus, to predict longer period motions, it is important to have a good estimate of the damping losses for the system of interest.

Figs. 5 and 6 compare the results of the small mass and large mass tests with their AMA predictions within the higher-frequency range of 225–425 non-dimensional Hertz.

Similar tests and calculations were performed on panels with up to three attached masses and they showed similar agreement.

4. Conclusions

Relations for the band-limited, high-frequency response of a panel with attached masses were summarized and verified by experiment. These relations describe the transverse displacement (velocity, etc.) of a panel when it is given a localized, impulsive excitation. These relations provide a reasonable approximation of the panel behavior in frequency ranges with significant modal content (i.e. high frequencies). The relations include the local panel response near an added mass or the load as well as the spatially averaged, mean-squared response. These relations are much simpler to evaluate than their classical counterparts and typically require 85–95% less computer memory and time.

Acknowledgements

The first author appreciates the help of the Institute of Mechanics, Moscow State University, Moscow, Russia for acting as host during part of this work. Support for this work was provided

by NSF Division of International Programs under grant 9803043, Susan Parris, Program Director and by the Arkansas Science and Technology Authority under grant 98-B-02, Herbert L. Monoson, Vice President of Research.

Appendix A. The mean, modal cross-product: $\bar{\psi}_{ij}$

The mean value for the cross-product of modes at different locations, $\bar{\psi}_{ij}$, was introduced in Eq. (29). This may be estimated without solving the eigenproblem by using sinusoidal panel mode shapes and recognizing that away from the panel edges the boundary conditions have little effect at high frequencies. The continuous approximation is made by replacing the discrete mode summation with a continuous integration in mode number space,

$$\bar{\psi}_{ij} \approx \frac{\int_A \sin(n_x \pi \xi_{ni}) \sin(n_y \pi \eta_{ni}) \sin(n_x \pi \xi_{nj}) \sin(n_y \pi \eta_{nj}) \, \mathrm{d}A}{\int_A \mathrm{d}A}. \tag{A.1}$$

The integrand may be recast into a more useful sum of cosine functions and integrated on the region shown in Fig. 7. It is easiest to perform the integral in n_y first as this can be done analytically. The limits of integration are determined by using the frequency-mode number relation (4) and the appropriate values of ω. The domain has two portions: to the left and right of n_x^*. Thus the limits of integration are

$$\left(\frac{\omega_{min}}{\gamma\pi^2} - \frac{n_x^2}{\gamma^2}\right)^{1/2} \leqslant n_y \leqslant \left(\frac{\omega_{max}}{\gamma\pi^2} - \frac{n_x^2}{\gamma^2}\right)^{1/2} : \; n_x < n_x^*, \tag{A.2}$$

$$1 \leqslant n_y \leqslant \left(\frac{\omega_{max}}{\gamma\pi^2} - \frac{n_x^2}{\gamma^2}\right)^{1/2} : \; n_x > n_x^*, \tag{A.3}$$

where n_x^* is determined from Eq. (4) with $n_y = 1$ and $\omega = \omega_{min}$. The first integration in n_y yields

$$\bar{\psi}_{ij} \approx \frac{\int_{n_x} (\bar{\psi}_{ny,1} + \bar{\psi}_{ny,2}) \, \mathrm{d}n_x}{\int_{n_x} \int_{n_y} \mathrm{d}n_y \, \mathrm{d}n_x} \tag{A.4}$$

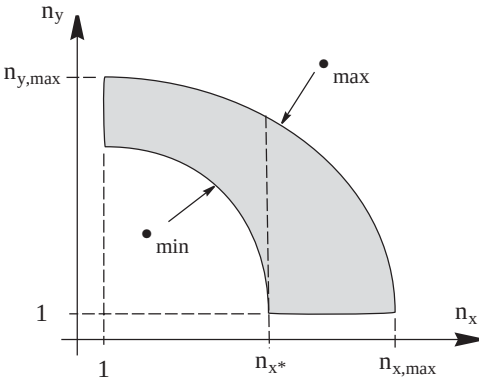

Fig. 7. The frequency range $\Delta\omega$ as seen in mode number space, n_x–n_y.

and

$$(\bar{\psi}_{ij})_{ny,1} = \left\{ \frac{\cos(n_x\pi\xi_i)\cos(n_x\pi\xi_j)}{\pi(\eta_j-\eta_i)(\eta_j+\eta_i)} \right\} [\Upsilon(\eta_j,\eta_i,\omega_{max}) - \Upsilon(\eta_i,\eta_j,\omega_{max}) - \Upsilon(\eta_j,\eta_i,\omega_{min}) + \Upsilon(\eta_i,\eta_j,\omega_{min})], \tag{A.5}$$

$$(\bar{\psi}_{ij})_{ny,2} = \left\{ \frac{\cos(n_x\pi\xi_j)\cos(n_x\pi\xi_i)}{\pi(\eta_j-\eta_i)(\eta_j+\eta_i)} \right\} + [\eta_i\cos(\pi\eta_j)\sin(\pi\eta_i) - \eta_j\cos(\pi\eta_i)\sin(\pi\eta_j) + \Upsilon(\eta_j,\eta_i,\omega_{min}) - \Upsilon(\eta_i,\eta_j,\omega_{max})], \tag{A.6}$$

where

$$\Upsilon(\eta_a,\eta_b,\omega_c) = \eta_a \sin\left(\eta_a\sqrt{\frac{\gamma\omega_c-(n_x\pi)^2}{\gamma^2}}\right) \times \cos\left(\eta_b\sqrt{\frac{\gamma\omega_c-(n_x\pi)^2}{\gamma^2}}\right). \tag{A.7}$$

Eq. (A.4) must then be integrated over n_x and, while it appears to be intractable analytically, the integrand is very well-behaved and can be done easily using a rudimentary numerical integration over the following limits:

$$\text{for} \quad \bar{\psi}_{ny,1}\colon\ 1 < n_x < n_x^*, \tag{A.8}$$

$$\text{for} \quad \bar{\psi}_{ny,2}\colon\ n_x^* < n_x < \left[\frac{\gamma\omega_{max}}{\pi^2} - \gamma^2\right]^{1/2}. \tag{A.9}$$

The trivial case of two coincident points is simply $\bar{\psi}_{ii} = \bar{\psi}^2 \approx \langle \psi^2 \rangle$.

References

[1] R.H. Lyon, Statistical Energy Analysis of Dynamical Systems: Theory and Applications, The MIT Press, Cambridge, MA, 1975.

[2] E.H. Dowell, Y. Kubota, Asymptotic modal analysis and statistical energy analysis of dynamical systems, American Society of Mechanical Engineers Journal of Applied Mechanics 52 (1995) 949–957.

[3] Y. Kubota, E.H. Dowell, Experimental Investigation of asymptotic modal analysis for a rectangular plate, Journal of Sound and Vibration 106 (2) (1986) 203–216.

[4] Y. Kubota, S. Sekimoto, E.H. Dowell, The high-frequency response of a plate carrying a concentrated mass, Journal of Sound and Vibration 138 (1990) 321–333.

[5] A.E. Sepulveda, H.L. Thomas, Improved transient response approximation for general damped systems, American Institute of Aeronautics and Astronautics Journal 34 (6) 1261–1269.

[6] M.L. Lai, A. Soom, Statistical energy analysis for the time-integrated transient response of vibrating systems, American Society of Mechanical Engineers Journal of Applied Mechanics 112 (1990) 206–213.

[7] E.C. Dalton, Ballistic shock response by an extension of statistical energy analysis, Proceedings, 63rd Shock and Vibration Symposium, 1992.

[8] R.J. Pinnington, D. Lednik, Transient statistical energy analysis of an impulsively excited, two oscillator system, Journal of Sound and Vibration 189 (1996) 249–264.
[9] R.R. Reynolds, E.H. Dowell, The transient response of structures using asymptotic modal analysis, American Society of Mechanical Engineers Journal of Applied Mechanics 65 (1) (1998) 258–265.
[10] R.R. Reynolds, The approximate, high frequency response of a panel with attached masses, Proceedings, 2000 ASME International Mechanical Engineering Congress & Exposition. Orlando, FL, November 5–10, 2000.